Available online at www.sciencedirect.com
SCIENCE DIRECT®
Journal of Crystal Growth 269 (2004) 218–228
JOURNAL OF CRYSTAL GROWTH
www.elsevier.com/locate/jcrysgro

Growth of GaAs crystals from Ga-rich melts by the VCz method without liquid encapsulation

F.-M. Kiessling[a,*], P. Rudolph[a], M. Neubert[a], U. Juda[a], M. Naumann[a], W. Ulrici[b]

[a] *Institute of Crystal Growth, Max-Born-Str. 2, 12489 Berlin, Germany*
[b] *Paul Drude Institute for Solid State Electronics, Hausvogteiplatz 5-7, 10117 Berlin, Germany*

Received 10 March 2004; accepted 23 April 2004

Available online 20 July 2004

Communicated by G. Müller

Abstract

The growth experiments and properties of undoped GaAs crystals grown by the vapour pressure controlled Czochralski (VCz) method without boric oxide encapsulant from Ga-rich melts are presented. Morphological and structural features were investigated by sensitive etching procedures. The precipitate content was analysed by laser scattering tomography. The mean scattering intensity of As precipitates decreases with increasing Ga excess in the melt. An enhanced probability of Ga-rich inclusion incorporation has been observed. In 3-in crystals, the mean etch pit density was decreased down to $5 \times 10^3\,cm^{-2}$ with improved radial homogeneity. The etch pits did not show cell patterning. Markedly reduced contents of boron and hydrogen have been detected. No oxygen defects and related complexes independently on the carbon concentration were ascertained by local vibrational mode. For the first time, the carbon concentration in the grown crystals was reduced by carefully controlling the CO content of the growth atmosphere in a VCz arrangement without boric oxide encapsulant. Such experiments without B_2O_3 encapsulant are of fundamental character and offer numerous information about the point defect situation in as-grown crystals.

PACS: 81.05.E; 81.10.F; 61.50.N; 61.72.F; 61.72.J; 81.30.M

Keywords: A1. Dislocations; A1. Point defects; A1. Precipitates; A2. Growth from melt; A2. Liquid encapsulated Czochralski method; A2. Vapor pressure controlled Czochralski method; B1. GaAs

1. Introduction

As is generally known the introduction of the liquid encapsulated Czochralski (LEC) technique to pull PbTe crystals by Metz et al. [1] in 1962 stands for the breakthrough in the melt growth of semiconductor compounds. For the first time Mullin et al. [2] used this method to grow III–V crystals, like GaAs, InP and GaP in 1965. A liquid B_2O_3 layer floating on the melt surface acts as an impermeable liquid cover and prevents in combination with the inert gas counter pressure the loss

*Corresponding author. Tel.: +49-30-6392-3032; fax: +49-30-6392-3003.
E-mail address: kiessling@ikz-berlin.de (F.-M. Kiessling).

0022-0248/$ - see front matter © 2004 Elsevier B.V. All rights reserved.
doi:10.1016/j.jcrysgro.2004.04.124

of the volatile component, e.g. As or P, from the dissociated melt. Such liquid encapsulant getters impurities from the melt and interacts as a chemical communicator between the gaseous and fluid phases important for the control of the oxygen and carbon potential in the melt. Meanwhile, this LEC technology has matured to a well-established production method for III–V single crystals. Large semi-conducting (SC) and semi-insulating (SI) GaAs crystals with diameters up to 150 mm and defined optical and electrical parameters are grown with high reproducibility [3].

Typically, Czochralski growth of GaAs with boric oxide encapsulant proceeds under As-rich conditions. This stands to reason because the congruent melting composition is seen to be on the As-rich side of the phase diagram. Furthermore, it is difficult to adjust precisely the melt composition during the whole growth process due to the fact that gallium and arsenic can oxidise. The higher chemical affinity of gallium to oxygen and the higher vapour pressure of gallium oxides over liquid boric oxide compared to those of arsenic oxides leads to a loss of Ga from the GaAs melt and, therefore, to a continuous increase of the As-excess in the melt [4]. In consequence of this growth from As-rich melts the related deviation from stoichiometry in the solid phase yields to a high concentration of arsenic interstitials which, according to a model proposed by Hurle [5], also react with gallium vacancies on cooling the crystal to form the antisite defect As_{Ga} known as EL2. Due to its sufficiently high concentration ($\approx 1–2 \times 10^{16}\,cm^{-3}$) this deep donor compensates the intentionally doped shallow acceptor carbon. To obtain SI material by this compensation mechanism the residual donor and acceptor impurity concentrations have to be low enough. One also has to keep in mind that the EL2 concentration depends on the off-stoichiometry and decreases when growing from Ga-rich melts. No As_{Ga} are formed in crystals grown from a melt composition below 48.3 at% As [5].

There are some essential disadvantages of the LEC growth from As-rich melts. One of the most serious consequences is the condensation of the arsenic excess atoms in precipitates due to the retrograde solubility during crystal cooling [6]. The presence of such second-phase particles may affect markedly the wafer surface polishing process and also the optical and electronic device parameters. With the continuously increasing demand for defect-reduced wafers needed for the rapidly growing market of epitaxial-based devices, a drastic reduction in density and size of the arsenic precipitates or better their complete dissolution is desired. Thus, state-of-the-art GaAs requires a costly bulk or wafer post-growth annealing.

Moreover, the use of B_2O_3 offers certain crucial shortcomings. High-temperature non-linearity and related high dislocation densities are generated at the contact region between the growing crystal and B_2O_3. The presence of boric oxide encapsulant results in an unintentionally boron doping in the crystals that may affect native point defect formation processes as well as the electrical activation of implanted silicon in field effect transistors [7]. Further, the LEC growth of heavily silicon-doped crystals for optoelectronic devices is quite impracticable because of scum formation on the melt surface that may induce serious growth problems like twinning [8]. Simultaneously, the boron incorporation enhances due to a reaction of the silicon in the melt with the boric oxide [9]. The boric oxide encapsulant also prevents an in situ control of the melt composition via the partial vapour pressure of the volatile component. Finally, no low-temperature gradients and, therefore, no dislocation-reduced crystal growth is possible by conventional LEC. The reason for that is the lacking heat protection of the growing crystal if it emerges from the encapsulant into the furnace atmosphere. A selective evaporation of the volatile component from the crystal surface takes place. There are persistent efforts to improve the Czochralski growth process for GaAs (InP) from the beginning.

In principle, the attempts to grow GaAs by the Czochralski technique without boric oxide encapsulant are not new and go back to the fifties. Gremmelmaier [10] described a GaAs hot-wall Czochralski (HWC) technique using a gas-tight

container made of fused silica. The inner walls were kept sufficiently hot (>620°C) in order to prevent the condensation of arsenic on them and to maintain a constant arsenic partial pressure against dissociation from the melt. A magnetic levitation system was applied for seed and crucible motion without any mechanical lead-throughs, which was somewhat later also adopted and sophisticated by Steinemann and Zimmerli [11]. Instead of such a relatively complicated technique, various systems with liquid seals (molten metals, B_2O_3), allowing the application of mechanical lead-throughs, were proposed by Richards [12], Tanenbaum [13], Mullin et al. [14], and Leung and Allred [15]. For the first time Baldwin et al. [16] applied a separately heated As source in a Czochralski hot-wall chamber to control in situ the As partial pressure over the uncovered melt. During the eighties the HWC technique with As source was advanced by Nizhizawa's group. Due to much lower-temperature gradients inherent to the hot-wall system, near-stoichiometric low-dislocation 3-in GaAs crystals with medium etch pit densities (EPDs) of about $10^4\,cm^{-2}$ were successfully grown [17]. During the nineties the HWC technique without B_2O_3 encapsulant receded somewhat into the background and was only used exclusively [18].

Instead of that the vapour pressure controlled Czochralski (VCz) growth with conventional B_2O_3 encapsulation has been matured [19,20]. This technique combines an inner hot-wall chamber to achieve low-temperature gradients and a stand-alone heated As source to control the arsenic fugacity in the process gas atmosphere in order to avoid dissociation at the surface of the grown crystal. Such growth mode is primarily aimed at the pulling of low-dislocation crystals. As usual, the melt composition cannot be controlled in situ and the crystal composition always deviates from the stoichiometry, which results in the above-described undesired arsenic precipitation process.

Recently, we took up again the idea of Czochralski growth of GaAs without encapsulant. We could invest our long-term experiences on VCz development on a markedly improved construction level [20] compared to the eighties.

2. Experimental procedure

2.1. Crystal growth

Fig. 1 shows the schematic drawing of the applied growth principle. The main constructive feature is an inner chamber made of graphite. It shields the growing crystal as well as its surrounding hot gas from the water cooled walls of the outer high pressure vessel. The thermal shielding function of the inner chamber yields to markedly reduced temperature gradients in axial and radial directions. Special solid sealings for the feed through mechanisms were developed [21]. The B_2O_3 encapsulant was completely omitted. The melt composition was controlled via the gas atmosphere by the arsenic partial pressure over their free melt surface. The arsenic pressure was adjusted by the temperature of the arsenic source in the chamber lid. The temperature could be varied within the range of 540–650°C corresponding to an arsenic pressure between 0.02 and 0.21 MPa. All sites of the inner chamber wall were kept at higher temperatures than the one of the As sources. In this way, we controlled the melt in situ from Ga-rich to near-stoichiometric compositions that is the region on the left side from the congruent melting point in the GaAs phase

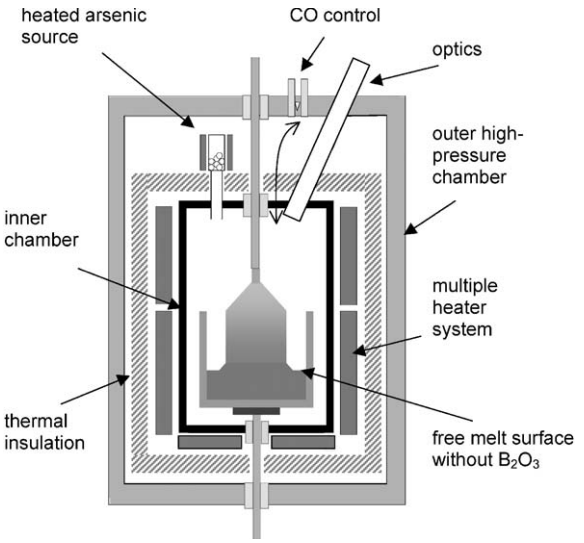

Fig. 1. Schematic sketch of the VCz crystal growth arrangement without boric oxide encapsulant.

diagram (note from a given source temperature the melt composition cannot be defined precisely due to the temperature gradient acting along the free melt surface). By weighing the separated Ga excess of the residual last-to-freeze crucible charge a related composition variation of the liquid-phase $Ga_{1-y}As_y$ from $y \approx 0.45$ to 0.50 could roughly be estimated for all our experiments.

Removing the B_2O_3 encapsulant, the tendency for dendrite growth increases due to the dramatically reduced radial temperature gradient. The crystals extremely tend to generate markedly enlarged facets showing the two-fold symmetry of the [0 0 1] direction in zinc blende structure. Thus, for growth without boric oxide the temperature field and heat fluxes within the growth chamber had to be reconfigured compared to a conventional VCz alignment. After optimisation based on assisting global computer modelling with codes CrysVUN++ and STHAMAS, the radial and axial temperature gradients at the growing interface were 3–5 and 20 K cm^{-1}, respectively. As shown in the drawing of Fig. 2a, slightly convex isotherms without concave parts were adjusted in the growing crystal to ensure growth without dislocation bunching. Analyses of growth striations revealing the shape of the crystal–melt interface confirmed these calculations. We also observed enhanced probability of twinning at growth from Ga-rich melts compared to As-rich one [22].

For the first time in such experiments without boric oxide encapsulant, the carbon concentration could be reduced markedly by using the controlling gas mode already described earlier [23]. Up to now there was no experimental evidence whether the presence of the boric oxide layer is necessary for this process.

2- and 3-in crystals were grown from pBN and fused silica crucibles in the [0 0 1] direction with a pulling rate of 5 mm h^{-1}. The crucible was automatically moved upwards to fix the position of the melt surface during growth. All crystals were cooled down to room temperature at rates of 25–50 K h^{-1}. Fig. 2b shows the image of a crystal grown without boric oxide encapsulant from a Ga-rich melt adjusted by a constant As a source temperature of 590°C. All crystals showed lustrous surfaces which were free of symptoms of dissociation.

2.2. Characterisation

The as-grown crystals were cut in slices with a thickness of 1–5 mm parallel and perpendicular to the growth direction in order to characterise longitudinal and radial parameter distributions. Second-phase particle analyses (precipitates, inclusions) were made by optical microscopy, IR laser scattering tomography (LST) and energy dispersive X-ray (EDX) spectroscopy. All samples were

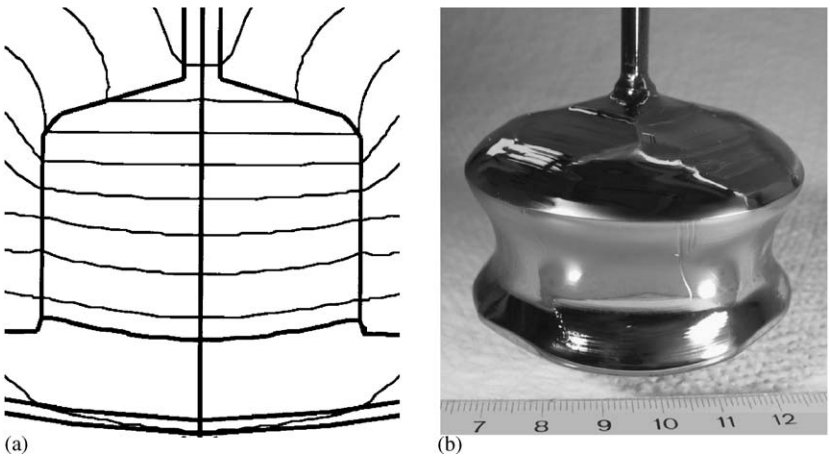

Fig. 2. (a) Drawing of isotherm shapes of a 3-in GaAs crystal calculated by global simulation with code CrysVUN++. The isotherms are plotted in steps of 25 K. (b) Image of a facetted GaAs crystal grown without B_2O_3 encapsulant.

analysed under identical LST conditions. For analyses of inclusions and striations, longitudinal slices cut parallel to the growth axis along the ⟨1 0 0⟩ direction were etched by diluted Sirtl with light (DSL). The standard procedure of KOH melt etching at 390°C was used for EPD determination. The concentrations of residual impurities were detected by glow discharge mass spectrometry (GDMS). The boron concentration was additionally measured by secondary ion mass spectroscopy (SIMS). The content of important system-inherent elements like C, O, N and H was evaluated from their local vibrational mode (LVM) absorptions measured at liquid nitrogen temperature. The $EL2^0$ concentration was ascertained by near IR absorption measurements. The electrical properties were obtained from Hall and conductivity measurements at room temperature.

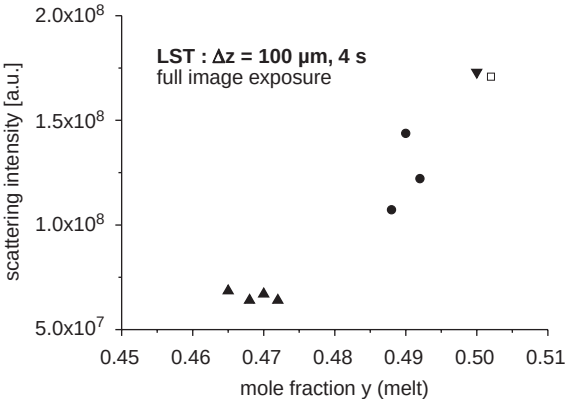

Fig. 3. Scattering intensities from precipitates in crystals grown without B_2O_3 from different melt compositions $Ga_{1-y}As_y$. The open symbol represents a conventional VCz crystal grown with B_2O_3. The error bar for the mole fraction y is within 0.003. For all measurements identical LST conditions were used.

3. Results and discussions

3.1. Second-phase analysis – precipitates and inclusions

Fig. 3 shows the scattering intensities from precipitates of undoped crystals grown from uncovered near-stoichiometric and Ga-rich melts. For comparison, the scattering value from a conventional VCz crystal grown from a slightly As-rich melt with B_2O_3 encapsulant and with the same temperature history is added. Hence, the scattering intensities only depend on the off-stoichiometry and decrease significantly with increasing Ga content in the melt. In accordance with this a reduction of the degree of decoration along the existing dislocations was observed. This type of scatterers could not be ascertained by LST in a crystal which was grown from a melt with a mole fraction of $y \approx 0.45$ at the most that contradicts the typical feature of GaAs crystals grown from As-rich melts [22]. We attribute the scatterers to different contents of arsenic precipitates [24,25]. Fornari et al. [26] analysed Si-doped GaAs LEC crystals grown from Ga-rich melts by TEM. They also reported drastic reductions in the density and in the size of As precipitates down to $3 \times 10^6\,cm^{-3}$ and 40 nm, respectively, in crystals grown from a melt of $y \approx 0.43$. Usually, the density of precipitates in LEC crystals grown from As-rich melts has been determined to 10^8–$10^9\,cm^{-3}$ and their sizes to 100–120 nm [27–29]. Obviously, melt compositions less or around a mole fraction of $y \approx 0.45$ yield to near-stoichiometric crystals without essential precipitation which is in good agreement with the value predicted by Hurle [5]. He concluded that a stoichiometric crystal is obtained when growing it from a Ga-rich melt of 44.8 at% As. This result also falls short of Wenzl's observations after which stoichiometric crystals have been obtained at $y = 0.47$ [30]. At this point of our investigation, it cannot yet be decided whether the phase extent of undoped GaAs is completely located on the As-rich side as calculations of Jurisch and Wenzl [31] showed or whether it is slightly overlapping the stoichiometric composition towards the Ga-rich side.

We found that the growth from such Ga-rich melts drastically increases the incorporation probability of Ga-rich inclusions. Images of a DSL etched crystal show that they act as typical second-phase inclusions and are surrounded by an enhanced EPD (Fig. 4). This seems to be caused by the misfit strain at the boundary to the crystal matrix. Their diameters are of some hundred micrometers, that is three orders of magnitude larger than the one of the precipitates. We

determined the inclusion composition in a scanning electron microscope by EDX mode to be gallium. Note it is important to distinguish between precipitation and inclusion genesis. Due to the retrograde solidus of the existence region, precipitates are formed during moderate cooling from point defect condensation (As interstitials). In contradiction to this process, inclusions are originated by melt-solution droplet capture at the growing melt–solid interface, e.g. if a Ga-enriched diffusion boundary layer is adjacent to the crystallisation front. Such inclusions follow the propagating interface, i.e. they move towards the higher temperature by the travelling solvent mechanism [20,30]. We ascertained such traces behind all inclusions as can be seen from Fig. 5a. Preferred sites for their incorporation are concave and morphological instable interface regions with re-entrant angles. In fact, we detected features of slightly facetted growth morphology (Fig. 5b). Similar images were published for GaAs [32] and for Ga-doped Ge single crystals [33]. At present, we attribute their incorporation in the crystal to an overcritical v/G ratio at the crystallisation front, with v the growth rate and G the temperature gradient, leading in low-temperature gradient growth from Ga-rich melts to morphological

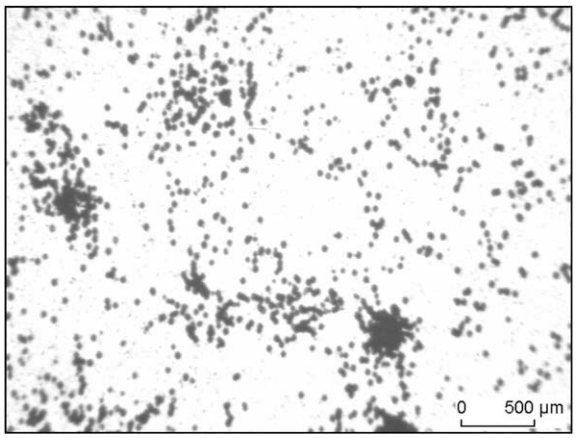

Fig. 4. Dislocation distribution with markedly enrichment of the EPD around inclusions. The crystal was grown from a Ga-rich melt with $y \approx 0.45$.

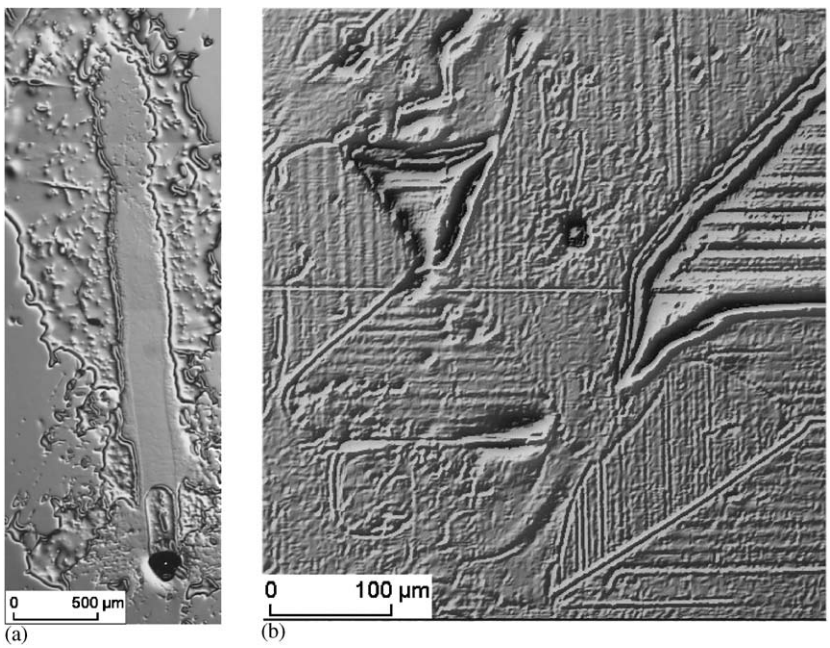

Fig. 5. Images of DSL etched samples: (a) longitudinal {1 0 0} section showing the trace of a migrated Ga-rich liquid droplet which finally solidified (dark blob), (b) viewing on a {1 0 0} wafer normal to the growth direction of a GaAs crystal grown from a melt with $y \approx 0.45$. The image shows striation patterns of a section through the growing pyramids formed of micro-facets.

instabilities. Already Wenzl mentioned the appearance of Ga inclusions with diameters of about 200 μm in crystals grown by HWC at As source temperatures below 600°C and pulling rates of $8\,mm\,h^{-1}$ [30].

Further investigations to optimise the growth conditions in order to drastically reduce or better avoid Ga inclusions are required.

3.2. Dislocations

At the beginning of our growth experiments two important questions arose: (i) is there any improvement of the radial dislocation distribution if the B_2O_3 layer is omitted, and (ii) does the dislocation density correlate with different melt compositions and, hence, with the deviation from stoichiometry of the grown crystal? In fact, we found a slightly improved radial EPD homogeneity. The density variations between edge and centre of these wafers are lower in comparison with those of VCz crystals grown with boric oxide (Fig. 6). No influence of the absence or presence of the boric oxide encapsulant on the shape of the dislocation distribution within the crystal was observed. Their shape reminds more of that of a "U" than a "W" and is typical for all crystals grown and cooled in low-temperature gradients with (VCz [20]) and without boric oxide encapsulant (HWC [17], horizontal boat [34]) and is attributed to the improved temperature field.

Fig. 6b shows that the density of etch pits also depends on the crystal composition. Growing crystals from melts with higher Ga contents, the dislocation density can be decreased. In agreement with our observations relatively low EPD values have also been detected in near-stoichiometric HWC crystals grown under controlled arsenic partial pressure [17]. Up to now our best average EPD in a crystal grown from a Ga-rich melt with $y \approx 0.45$ was measured to $5.4 \times 10^3\,cm^{-2}$. The most remarkable feature of this crystal is the absence of cellular patterning and even the formation of uncompleted cell walls (Fig. 4). Both effects can be explained by a minimisation of the intrinsic point defect content which otherwise acts as source of dislocation climbing in non-stoichiometric, i.e. arsenic-rich, crystals. As we demonstrated earlier, point defect assisted dislocation movement plays an important role in dislocation multiplication and even in cell wall formation [35].

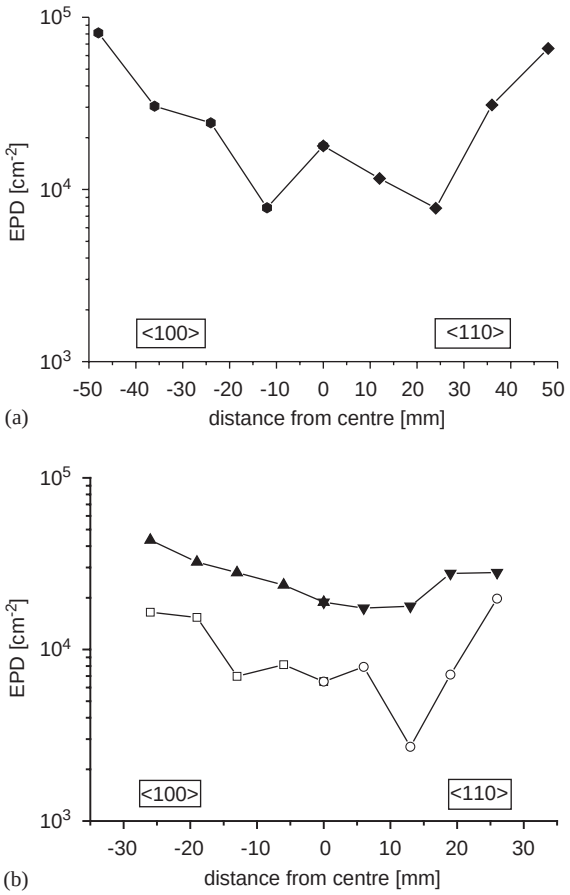

Fig. 6. EPD distribution along the radius in VCz crystals grown (a) with boric oxide encapsulant, (b) without B_2O_3 from melt compositions of $y \approx 0.50$ (full symbol) and $y \approx 0.47$ (open symbol). The mean EPD decreases with decreasing off-stoichiometry.

3.3. Residual impurities

In Table 1 selected information of the growth conditions and properties of typical VCz crystals (V1–V7) grown in the same chamber, the GaAs starting material (S1) and the used arsenic source material (S2) are compiled. A lot more crystals were grown but only one typical crystal of certain

Table 1
Selected impurity concentrations and properties of GaAs crystals grown by the VCz method with (V1) and without B_2O_3 encapsulant (V2–V7) at different arsenic source temperatures in comparison to the starting material (S1) and As source material (S2)

Sample	B_2O_3	Process gas	P_{CO} (mbar)	Crucible	Arsenic source temperature (°C)	$EL2^0$ (cm^{-3}) IR	B (cm^{-3}) SIMS GDMS*	C_{As} (cm^{-3}) LVM GDMS*	Si (cm^{-3}) GDMS	S (cm^{-3}) GDMS	Carrier type and concentration (cm^{-3})
V1	Yes	Ar	10	pBN	615	8.3 E15	1.8 E16	8 E14	2 E15	1 E15	n = 2 E07
V2	No	Ar	> 70	SiO_2	590	n.d.[a]	2 E15	2.5 E16	5.3 E16	2.9 E16	n = 2.6 E16
V3	No	Ar	> 70	pBN	630	n.d.[b]	8 E15	3.5 E16	1 E15	6 E15	p = 1.4 E16
V4	No	Ar	6.7	pBN	630	8.0 E15	—	8.0 E15	8 E15	6.2 E16	n = 1.6 E16
V5	No	Ar	1.9	pBN	630	1.3 E16	9 E15	1.3 E15	6 E14	4 E15	n = 7 E13
V6	No	N_2	> 70	pBN	590	8.0 E15	1 E15	6.3 E15	2 E14	2 E15	n = 8 E06
V7	No	N_2	1.5	pBN	630	8.0 E15	4 E15	9 E14	2 E14	6 E15	n = 6 E14
S1							5 E17*	2 E15*	4 E14	4 E14	
S2							2 E15*	1 E17*	2 E15	6 E14	

Note: The error bar of the CO partial pressure is $< \pm 10\%$. Lower arsenic source temperature corresponds to a higher Ga content in the melt (note: n.d.—not detectable $EL2^0$ concentration means below $2 \times 10^{15}\,cm^{-3}$ and is due to (a) Si-doping (b) p-conductivity). The error bars of GDMS and SIMS are $< \pm 20\%$ and $< \pm 10\%$, respectively.

growth conditions in each case was chosen. For reasons of comparison a crystal (V1) under conventional growth conditions (B_2O_3 encapsulant with 200 ppm water content) was pulled. Three crystals were grown without carbon control, one (V2) from a fused silica crucible, two others (V3, V6) from a pBN crucible. Crystals V4, V5 and V7 were also grown out of pBN crucibles but with in situ control of the CO concentration in the process gas.

The crystals grown without boric oxide (V2–V7) show reduced boron contents of about one order of magnitude compared to crystals which were grown with a B_2O_3 encapsulant, though it should be noted that the boron concentration in this special crystal V1 is comparatively low. Except the boron concentration in crystals V6 and V7 the lowest boron contents were always detected in crystals grown from fused silica crucibles as seen in the one example. This can be explained by oxygen release from this crucible and a reaction with boron in the melt to form boric oxide. The reason for the lower boron content in the crystals V6 and V7, which were also grown from a pBN crucible, is to be found in the use of the nitrogen process gas resulting in a reaction with the residual boron impurities of the starting material (S1) to BN. Indeed, in case of nitrogen process gas we always observed a few small floating particles on the melt surface identified as BN by EDX. Growing under argon process gas no floating particles were observed and hence, a somewhat higher boron content was measured in those crystals (V3,V5).

The crystals grown from uncovered melts in the argon process gas and without carbon control (V2,V3) show always a markedly increased carbon concentration due to the inner chamber assemblies made of graphite. This is in accordance with the observations of Tomizawa et al. [36], who used a similar VCz arrangement. Crystal V3 is of p-type conductivity attributed to the shallow acceptor carbon against what sample V2 is of n-type conductivity due to the higher silicon than carbon concentration. The silicon is incorporated from the fused silica crucible and acts as compensating donor. Crystal V6 was also grown without carbon control but in nitrogen atmosphere. Surprisingly, the carbon content was reduced compared to the crystals V2 and V3. It is known from growth experiments with boric oxide that the nitrogen fugacity influences the chemical potential of oxygen and can finally reduce the carbon concentration [37]. From our present data, we cannot yet verify whether the reduced carbon concentration can only or at all be attributed to the influence of the nitrogen.

The enhanced incorporation of C at growth without encapsulant can mainly be attributed to

high CO fugacity in the gas phase. CO gas is released by the reaction of residual water with graphite according to $C + H_2O \leftrightharpoons CO + H_2$ and due to the Boudouard equilibrium $CO_2 + C \leftrightharpoons 2CO$. Growing crystals without B_2O_3 the H_2O comes probably from the moisture in the air adsorbed in the inner graphite assemblies of the VCz chamber and the process gas. Besides a possible direct absorption of carbon species by the GaAs melt surface unbounded carbon can also be produced by the reactions $CO + 2Ga \leftrightharpoons C + Ga_2O$ and $3CO + 2Ga \leftrightharpoons 3C + Ga_2O_3$ at the melt–gas interface.

To reduce the carbon content and adjust the electrical properties of the growing crystal, we used the in situ control of the CO content by gas stream control. In such crystals, the carbon concentration was adjusted by a certain fixed CO partial pressure (e.g. V4). At a much lower CO fugacity but similar for both crystals V5 and V7 the carbon concentration could be reduced of about one order of magnitude down to low $10^{15}\,cm^{-3}$ independently of the used process gas. By applying the nitrogen inert gas the carbon concentration in crystal V7 could be reduced even below $1 \times 10^{15}\,cm^{-3}$. The data are not significant enough to attribute these different carbon concentrations to the influence of the gas type. Only by fixing the CO content in the process gas carbon cannot be incorporated homogeneously in the growing GaAs crystal. We observed a slightly increasing axial carbon concentration which cannot simply be described by the Scheil equation applying an effective distribution coefficient of $1 < k_e < 2$ [38]. Such incorporation behaviour is noted for a non-conservative system [39] acting in our arrangement too.

Surprisingly, samples V4 and V7 showed SC behaviour of n-type conductivity, which we attributed to donor impurities probably sulphur according to the GDMS analyses. Against it V6 shows SI behaviour due to a lower sulphur content. To clarify the origin of the enhanced S content which does not come from the melt or the starting material (see V1 and S1 in Table 1) the As source materials were investigated. No enhanced sulphur concentration was detected by GDMS. We assume that the undesired sulphur comes from the chamber assemblies.

The causes of non-detectable $EL2^0$ concentrations for two growth regimes represented by the samples V2 and V3 are different. In the case of V2, the silicon donor prevents the formation of EL2 probably at all due to the known strong dependence of the As_{Ga} concentration on the free-electron concentration [40] but in the sample V3 one certainly can expect to detect the antisite defect. Due to the relatively high carbon concentration almost all antisites are in the charge state $EL2^{2+}$.

In all crystals grown without B_2O_3 no oxygen defects and related complexes could be detected by LVM analysis nor in such crystals which were grown from fused silica crucibles or either from Ga_2O_3-doped melts. Surprisingly, we found in all these examples H-related complexes even though their content is smaller by a factor of 10–100 compared to crystals grown with encapsulant. The detected complexes are, e.g. Si_{Ga}–H in n-type GaAs and C_{As}–H in p-type GaAs. In the semi-insulating GaAs samples, we observed the N_{As}–H LVM at $2947.4\,cm^{-1}$ and the LVM lines due to the Z–H complex [41]. No other known hydrogen-impurity complexes could be detected.

No substitutional isolated nitrogen (N_{As}) with concentrations higher than the detection limit of $7 \times 10^{15}\,cm^{-3}$ could be detected by LVM. In crystals grown in N_2 atmosphere, the [N_{As}–V_{Ga}] complex has been ascertained [42]. The LVM lines of 1244 and $1325\,cm^{-1}$, caused by two different B-N defects, were not found in crystals grown without B_2O_3 independently, whether they were pulled in N_2 or Ar atmosphere. This result confirms the measured low boron concentration by SIMS and the markedly reduced probability to form such defects.

Up to now we could not correlate clear effects of the reduced boron concentration on any other as-grown defect concentrations in these GaAs crystals even though we have determined differences in some point defect concentrations to comparable GaAs material grown with boric oxide. First results on dependencies of vacancy concentrations on the deviation from stoichiometry were already published elsewhere [43].

4. Conclusions

GaAs crystals have been grown from Ga-rich melts by the VCz method under controlled As partial pressure and without boric oxide encapsulant. This technique is not new and was introduced as HWC mode even before the LEC method was used. The growth of GaAs crystals without B_2O_3 encapsulant offers the possibility to study the influence of the B_2O_3, usually used as pressure cover in conventional production techniques, like LEC and VB (vertical Bridgman), on the material properties. Using this growth arrangement numerous methodical studies not only about structural characteristics but also about the point defect situation in as-grown crystals can be undertaken. The temperature control of the stand-alone arsenic source allows an in situ control of the melt composition and, hence, the point defect content in the grown crystal.

We found that nearly arsenic precipitate-free crystals can be grown from melts with compositions $\leqslant 45$ at% As. In such samples no dislocation decoration by arsenic precipitates could be observed. However, the probability of Ga-rich inclusion incorporation increases drastically in such crystals and the v/G ratio has to be optimised in future experiments.

The average EPD decreases with decreasing deviation from stoichiometry. A reduction of the mean dislocation density down to values of around $5 \times 10^3\,\mathrm{cm}^{-2}$ without features of cell patterning were observed in crystals grown from melt with $y \approx 0.45$. The homogeneity of the radial distribution is improved due to the missing B_2O_3 layer that introduces mechanical stress in conventional GaAs crystals grown by LEC and VCz techniques.

Crystals grown without B_2O_3 show markedly reduced contents of boron and hydrogen. An interesting result is that no oxygen defects and related complexes independently on the carbon concentration were detectable. Without controlling the CO potential in the gas phase the carbon concentration is markedly enhanced. For the first time at VCz growth without encapsulant the carbon concentration in the GaAs crystals could be decreased down to a level of $\sim 10^{15}\,\mathrm{cm}^{-3}$ by using the gas flow control.

Acknowledgements

The authors are grateful to M. Czupalla and M. Pietsch for growing the crystal with boric oxide, Dr. Ch. Frank-Rotsch for numerical modelling, B. Lux, Th. Wurche and M. Imming for wafer preparation, H. Baumüller for EPD analysis, Dr. P. Wilde for EDX analysis, and Dr. K. Irmscher for electrical measurements. The work was supported by the German Research Association under contract numbers RU 505/10-1 and 10-2 and partially by the Freiberger Compound Materials GmbH.

References

[1] E.A.P. Metz, R.C. Miller, R. Mazelsky, J. Appl. Phys. 33 (1962) 2016.
[2] J.B. Mullin, B.W. Straughan, W.S.J. Brickell, Phys. Chem. Solids 26 (1965) 782.
[3] P. Rudolph, M. Jurisch, in: H.J. Scheel, T. Fukuda (Eds.), Crystal Growth Technology, Wiley, West Sussex, 2003, p. 293.
[4] M. Jurisch, in: P. Kiesel, S. Malzer, T. Marek (Eds.), Proceedings of the Symposium on Non-Stoichiometric III–V Compounds, Physik mikrostrukturierter Halbleiter Bd.6, Erlangen-Nürnberg, Friedrich-Alexander-Universität, 1998, p. 135.
[5] D.T.J. Hurle, J. Appl. Phys. 85 (1999) 6957.
[6] P. Rudolph, Cryst. Res. Technol. 38 (2003) 542.
[7] S. Okubo, Y. Otoki, M. Watanabe, S. Kuma, Jpn. J. Appl. Phys. 32 (1993) 1898.
[8] B. Cockayne, W.R. MacEwan, D.A.O. Hope, I.R. Harris, N.A. Smith, J. Crystal Growth 87 (1988) 6.
[9] K. Hashio, S. Sawada, M. Tatsumi, K. Fujita, S. Akai, J. Crystal Growth 173 (1997) 33.
[10] R. Gremmelmaier, Z. Naturforsch. 11a (1956) 511.
[11] A. Steinemann, U. Zimmerli, in: H.S. Peiser (Ed.), Crystal Growth, Pergamon Press, Oxford, 1967, p. 81.
[12] J.L. Richards, J. Sci. Instrum. 34 (1957) 289.
[13] M. Tanenbaum, in: N.B. Hannay (Ed.), Semiconductors, Reinhold, New York, 1959.
[14] J.B. Mullin, W.R. MacEwan, C.H. Holliday, A.E.V. Webb, J. Crystal Growth 13/14 (1972) 629.
[15] P.C. Leung, W.P. Allred, J. Crystal Growth 19 (1973) 356.
[16] E.M.C. Baldwin, J.C. Brice, E.J. Millet, J. Sci. Instrum. 42 (1965) 883.
[17] K. Tomizawa, K. Sassa, Y. Shimanuki, J. Nishizawa, Inst. Phys. Conf. Ser. No. 91 (1988) 435.
[18] A. Dahlen, A. Fattah, H. Wenzl, B. Wiedemann, A. Winnaker, in: Abstracts, ICCG-XI, The Eleventh International Conference on Crystal Growth, The Hague, June 18–23, 1995, p. 337.

[19] M. Tatsumi, K. Fujita, in: M. Isshiki (Ed.), Recent Developments of Bulk Crystal Growth, Research Signpost, Trivandrum, 1998, p. 47.
[20] M. Neubert, P. Rudolph, Prog. Cryst. Growth Charact. Mater. 43 (2001) 119.
[21] H. Trompa, M. Neubert, M. Seifert, P. Krause, P. Rudolph, M. Jurisch, P. Prause, Patent Description DE 196027 C1, 1996.
[22] D.T.J. Hurle, J. Crystal Growth 147 (1995) 239.
[23] K. Jacob, Ch. Frank, M. Neubert, P. Rudolph, W. Ulrici, M. Jurisch, J. Korb, Cryst. Res. Technol. 35 (2000) 1163.
[24] J.L. Weyher, C. Frigeri, L. Zanotti, H. Ch Alt, P. van der Wel, P. Gall, Seventh Conference Semi-Insulating III–V Materials, Ixtapa, Mexico, 1992, p. 97 (Chapter 3).
[25] T. Steinegger, M. Naumann, M. Jurisch, J. Donecker, Mater. Sci. Eng. B 80 (2001) 215.
[26] R. Fornari, C. Frigeri, R. Gleichmann, J. Electron. Mater. 18 (1989) 185.
[27] A.G. Cullis, P.D. Augustus, D.J. Stirland, J. Appl. Phys. 51 (1980) 2556.
[28] P. Schlossmacher, K. Urban, H. Rüfer, J. Appl. Phys. 71 (1992) 620.
[29] J.L. Weyher, T. Schober, K. Sonnenberg, P. Franzosi, Mater. Sci. Eng. B 55 (1998) 79.
[30] H. Wenzl, W.A. Oates, K. Mika, in: D.T.J. Hurle (Ed.), Handbook of Crystal Growth, Vol. 1, North-Holland, Amsterdam, 1993, p. 103.
[31] M. Jurisch, H. Wenzl, Workshop of the German Ass. on Crystal Growth (DGKK) on Simulations in Crystal Growth, Memmelsdorf, October 2002.
[32] J.L. Weyher, J. van de Ven, J. Crystal Growth 78 (1986) 191.
[33] D.T.J. Hurle, B. Cockayne, in: D.T.J. Hurle (Ed.), Handbook of Crystal Growth 2: Bulk Crystal Growth, Elsevier, Amsterdam, Tokyo, 1994, p. 130.
[34] J. Lagowski, H.C. Gatos, D.G. Aoyama, Lin, Appl. Phys. Lett. 45 (1984) 680.
[35] M. Naumann, P. Rudolph, M. Neubert, J. Donecker, J. Crystal Growth 231 (2001) 22.
[36] K. Tomizawa, K. Sassa, Y. Shimanuki, J. Nishizawa, in: J. Chikawa, K. Sumino, K. Wada (Eds.), Defects and Properties of Semiconductors: Defect Engineering, KTK Sci. Publ., Tokyo, 1987, p. 25.
[37] K. Korb, T. Flade, M. Jurisch, A. Köhler, Th. Reinhold, B. Weinert, J. Crystal Growth 198/199 (1999) 343.
[38] N. Sato, M. Kakimoto, Y. Kadota, in: A. Milnes, C. Miner (Eds.), Sixth Conference Semi-Insulating III–V Materials, Adam Hilger Bristol, Toronto, 1990, p. 211.
[39] S. Eichler, A. Seidl, F. Börner, U. Kretzer, B. Weinert, J. Crystal Growth 247 (2003) 69.
[40] J. Lagowski, H.C. Gatos, J.M. Parsey, K. Wada, M. Kaminska, W. Walukiewicz, Appl. Phys. Lett. 40 (1982) 342.
[41] W. Ulrici, M. Jurisch, Physica B 308–310 (2001) 835.
[42] W. Ulrici, F.-M. Kiessling, P. Rudolph, Phys. Stat. Sol. (b) 241 (2004) 1281.
[43] F.-M. Kiessling, M. Neubert, P. Rudolph, W. Ulrici, Mater. Sci. Semicond. Proc. 6 (2003) 303.